GABA$_B$ receptor modulation of visual sensory processing in adults with and without Autism Spectrum Disorder

Running title: GABA$_B$ function in ASD.

Qiyun Huang[1,2]†, Andreia C. Pereira[1,2,3,4]†, Hester Velthuis[1,2], Nichol M. L. Wong[1,2], Claire L. Ellis[1,2], Francesca M. Ponteduro[1,2], Mihail Dimitrov[1,2], Lukasz Kowaleski[1,2], David J. Lythgoe[5], Diana Rotaru[5], Richard A. E. Edden[6,7], Alison Leonard[1,2], Glynis Ivin[8], Jumana Ahmad[9], Charlotte M. Pretzsch[1,2], Eileen Daly[1,2], Declan G. M. Murphy[1,2,10]‡, Gráinne M. McAlonan[1,2,10]‡*

† These authors contributed equally to this work.
‡ These authors contributed equally to this work.
* Corresponding author

[1]Department of Forensic and Neurodevelopmental Sciences, Institute of Psychiatry, Psychology & Neuroscience, King's College London, London, UK.
[2]Sackler Institute for Translational Neurodevelopment, Institute of Psychiatry, Psychology & Neuroscience, King's College London, London, UK.
[3]Coimbra Institute for Biomedical Imaging and Translational Research, University of Coimbra, Coimbra, Portugal.
[4]Institute of Nuclear Sciences Applied to Health, University of Coimbra, Coimbra, Portugal.
[5]Department of Neuroimaging, Institute of Psychiatry, Psychology & Neuroscience, King's College London, London, UK.
[6]Russel H Morgan Department of Radiology and Radiological Science, Johns Hopkins University School of Medicine, Baltimore, MD, USA.
[7]F. M. Kirby Research Center for Functional Brain Imaging, Kennedy Krieger Institute, Baltimore, MD, USA.
[8]South London and Maudsley NHS Foundation Trust Pharmacy, London, UK.
[9]School of Human Sciences, University of Greenwich, London, UK.
[10]MRC Centre for Neurodevelopmental Disorders, King's College London, London, UK.

*Corresponding author:
Professor Grainne M. McAlonan
Institute of Psychiatry, Psychology and Neuroscience (IoPPN)
King's College London
16 De Crespigny Park, Denmark Hill, London, SE5 8AF
Phone: +44 0207 848 0831
Email: grainne.mcalonan@kcl.ac.uk

Single Sentence Summary

Differences in GABAergic function are fundamental to autistic (visual) sensory neurobiology; but are modulated by targeting $GABA_B$.

Abstract

Sensory atypicalities in autism spectrum disorder (ASD) are thought to arise at least partly from differences in γ-aminobutyric acid (GABA) receptor function. However, the evidence to date has been indirect, arising from correlational studies in people and preclinical animal model systems. Here, we tested this hypothesis directly, in 44 adults (n = 19 ASD). Baseline (placebo) concentration of occipital lobe GABA+ (GABA plus co-edited macromolecules) were measured using proton Magnetic Resonance Spectroscopy (^{1}H-MRS). Steady-state visual evoked potential (SSVEP) elicited by a passive visual surround suppression paradigm was compared following double-blind randomized oral administration of placebo, 15 mg or 30 mg arbaclofen (STX209), a GABA type B ($GABA_B$) receptor agonist. In the placebo condition, the neurotypical SSVEP response was affected by both the foreground stimuli contrast and background interference (i.e. suppression). In ASD, however, all stimuli conditions had equal salience; and background suppression of the foreground response was weaker. Although there was no placebo group difference in GABA+, GABA+ concentration positively correlated with response to maximum foreground contrast during maximum background interference in neurotypicals, but not ASD. In neurotypicals sensitivity to visual stimuli was disrupted by 30 mg arbaclofen, whilst in ASD it was made more 'typical' and visual processing differences were abolished. Hence, differences in GABAergic function are fundamental to autistic (visual) sensory neurobiology; but are modulated by targeting $GABA_B$.

Introduction

Hyper- or hyporeactivity to sensory input is integral to the DSM-5 definition of autism spectrum disorder (ASD) (*1*); and sensory atypicalities have been considered at least a contributory cause of many of the behavioral features of ASD (*2, 3*). However, the range of sensory alterations in ASD is broad and their neurobiological basis is poorly understood; and to date no pharmacological interventions which target this (or any other) core ASD feature have been successfully developed.

For instance, in the visual modality, compared with neurotypicals, autistic individuals have been reported to have an enhanced local visual processing (*2*), a slower rate of binocular rivalry (*4*), reduced spatial suppression (*5*), and decreased global motion perception (*6*). In motion discrimination tasks especially, there is an emerging consensus that autistic participants have superior discrimination for large stimuli and less spatial suppression (*5, 7, 8*). Despite the diverse nature of findings, it has been suggested that at a neurobiological level differences in the regulation of excitatory (E) – inhibitory (I) balance, and especially inhibitory γ-aminobutyric acid (GABA) pathways, may contribute to altered visual sensory processes in ASD (*9-11*).

These studies were important first steps in describing the nature of atypical (visual) sensory processing in ASD and its potential inhibitory underpinnings (in terms of computational modeling). However, the neurobiological basis of autistic visual processing is less accessible, especially in the living human brain. Accumulating evidences have been found for autism-related alterations within inhibitory GABA pathways (*12-15*); but the picture is complicated. It has been

3

reported that absolute GABA concentration in the occipital cortex (measured using proton magnetic resonance spectroscopy; ^{1}H-MRS) are not altered in ASD (*16-20*), however, a correlation between GABA concentration and visual perceptual dynamics, as measured by binocular rivalry, has been demonstrated in neurotypicals but reported to be absent in ASD (*21*). GABAergic functional differences during visual processing have therefore been indirectly implicated in ASD (despite no differences in bulk measures of GABA) (*21*).

There is also evidence for atypicalities and the involvement of GABA in other sensory modalities in autism, particularly tactile/auditory domains (*22-25*). Here however, we aimed to build upon studies of visual processing in ASD and include a pharmacological probe of the GABA system.

Of the two sub-types of GABA receptors, GABA type A (GABA$_A$) receptors elicit a 'phasic' fast-acting post-synaptic inhibition and a 'tonic' extracellular inhibitory response (*26*). GABA type B (GABA$_B$) receptors coordinate 'slower' changes in neuronal excitability - but can also rapidly inhibit neural network activity (*27*). GABA$_B$ activation has also been shown to enhance the magnitude of the tonic GABA$_A$ current (*28*). This receptor 'cross-talk' may explain why, in the neurotypical brain, activation of either receptor subtype increases visual perceptual suppression during binocular rivalry (*29*). Although GABA receptors are critical for visual inhibitory processes, direct evidence supporting the hypothesis that GABA receptor activation modulates visual sensory differences in ASD is lacking.

Here, we aimed to directly test the hypothesis that altering GABA function

4

differentially alters (visual) sensory processing in people with and without ASD by pharmacologically challenging the GABA system. We acquired ^{1}H-MRS measures of occipital GABA concentration. Electroencephalogram (EEG) was used to record steady-state visual evoked potential (SSVEP) elicited by flickering stimuli at low and high contrast in the foreground of the peripheral visual field during the presence or absence of background interference (*30*). SSVEP amplitude has been shown to increase monotonically with the foreground contrast in neurotypicals (*31, 32*). Importantly, this paradigm does not rely upon high-order cognitive processes, complex verbal communication, or active responses; so reducing the influence of non-specific test demands on the results. Our first aim was to confirm a differential relationship between GABA and visual suppression mechanisms in people with and without ASD. Hence, we tested predictions that:

a) Background stimuli do not interfere with the foreground stimulus response in ASD (i.e. there would be weaker suppression compared to controls); and

b) Occipital GABA concentration correlate with response during background interference in the control group but not the ASD group.

We then carried out a 'rescue' experiment and compared SSVEP responses in autistic individuals and neurotypicals at baseline (placebo) and following an oral dose of arbaclofen (STX209). We chose arbaclofen because it is a selective $GABA_B$ receptor agonist which has been shown to be safe and well-tolerated in ASD (*33, 34*). We used placebo, a low (15 mg) and a higher (30 mg) dose of arbaclofen to better

understand dose-dependency and minimize the chance of false negatives as a result of selecting an inappropriate dose. This, we hoped, would generate Proof of Concept that boosting GABA 'rescues' visual processing differences in ASD.

Results

Foreword. Nineteen ASD (8 females) and 25 controls (13 females) were included and 94 study visits were completed: 38 placebo (P) visits (17 ASD, 21 controls), 30 low-dose (L) visits (13 ASD, 17 controls) and 26 high-dose (H) visits (14 ASD, 12 controls). Eleven ASD and 12 controls completed all three visits. Thus, there were six groupings by participant and drug dose: Control_P, Control_L, Control_H, ASD_P, ASD_L and ASD_H. Visits were at least one week apart to ensure complete drug wash-out.

Occipital concentration of GABA+ are comparable in adults with and without ASD.

We used Hadamard-Encoding and Reconstruction of Mega-Edited Spectroscopy (HERMES) (35) and LCModel v 6.3-1L (Stephen Provencher Inc., Oakville, Canada) to quantify occipital GABA+ (GABA plus co-edited macromolecules (36, 37)) at placebo within the medial occipital lobe (Fig. 1). Fifteen ASD (5 females) and 19 controls (10 females) in total had placebo GABA+ concentration available from a voxel located in the medial occipital cortex. One male control participant was excluded due to poor data quality, thus the final MRS sample included 15 ASD and

18 control participants. Please see Supplementary Materials for more details on GABA+ data availability. We did not observe group differences between controls and ASD participants in occipital placebo GABA+ concentration ($t_{(31)} = 0.33$, $p = 0.74$), as predicted based on prior literature. No drug effect or group x drug interaction was observed (Supplementary Fig. S1).

Visual sensory processing is altered at placebo in ASD.

In our paradigm, four flickering circular foreground gratings had a contrast of 0% (F0), 30% (F30) or 100% (F100); the background pattern was either uniform gray (B0) or vertical Gabor gratings with 100% contrast (B100) fused with foreground gratings spatially to induce maximum background interference (Fig. 2). Raw EEG data from six recording channels over the occipital lobe (i.e. Oz, O1, O2, POz, PO3 and PO4) were pre-processed and analyzed in MATLAB 9.2.0 (The Mathworks Inc., Natick, Massachusetts, USA) using in-house scripts (see Materials and Methods).

The dependent variable used in subsequent linear mixed-effects model (LMM) analyses was θ, which was defined to be the proportion of SSVEP increase elicited by a non-zero foreground contrast, referenced to the zero foreground contrast. For example, θ[F30, B100] represents the proportion of SSVEP increase under configuration 5 (Table 1), referenced to its corresponding zero foreground contrast under configuration 4. The reported *es* was the LMM estimated value. A support vector machine (SVM) model was also trained to classify between each pair of the six participant visit groups. For each participant visit, we extracted a 4-d feature vector of

θ from raw EEG signals which was used for SVM training process:

$$Features : \{\theta[F30, B100], \theta[F100, B100], \theta[F30, B0], \theta[F100, B0]\}$$

The average classification accuracy *ca* was determined by a 10-fold cross validation process, repeated by 10 times, its statistical significance assessed using (x10,000) permutation testing, thresholded at $p < 0.05$ (see Materials and Methods).

The scatter plots of θ values (with mean $\pm$ SE) of the six participant visit groups are shown in Fig. 3. For the two baseline groups Control_P and ASD_P (Fig. 3a, d), both LMM (Table 2) and SVM (Table 3) results confirmed the group difference in baseline (placebo) response patterns. Thus, in the Control_P group, we observed significant effect of both background interference and foreground contrast on θ (BI: es = -0.27, $p = 1.64 \times 10^{-6}$; FC: es = 0.17, $p = 0.002$). In ASD_P, neither background interference nor foreground contrast had a prominent effect on θ. Permutation testing of the SVM classification (see Materials and Methods) demonstrated that there was a significant group difference at placebo (ca = 70.5%, $p = 0.033$) and also at high dose arbaclofen (ca = 72.5%, $p = 0.021$).

Background interference suppressed SSVEP responses to F100 in controls but not in ASD.

To measure the suppression effect of background on SSVEP responses to foreground, we defined the effect of background interference on each foreground contrast condition as 'surround suppression' (SS):

(i) SS_{F30}: the difference in response to F30 with no background interference (B0) and F30 response during maximum background interference (B100);

$$SS_{F30} = \theta[F30, B0] - \theta[F30, B100] \qquad (1)$$

(ii) SS_{F100}: the difference in response to F100 with no background interference (B0) and F100 response during maximum background interference (B100);

$$SS_{F100} = \theta[F100, B0] - \theta[F100, B100] \qquad (2)$$

We confirmed that at placebo there was a significant group difference for SS_{F100} ($t_{(36)} = 3.02$, $p = 0.01$), but not for SS_{F30} ($t_{(36)} = 1.54$, $p = 0.13$). Please see Fig. 4. Thus, background interference suppressed SSVEP responses to F100 in the control group but not the ASD group.

SSVEP responses during background interference were correlated with GABA+ in the occipital lobe in controls but not in ASD.

We ran a correlation analysis to determine whether visual processing during background interference was related to occipital GABA+ concentration at placebo. The correlation scatter plots for both groups were shown in Fig. 5. In the control group, as predicted, there was initially a significant correlation between θ and the

concentration of GABA+ ($r_{(18)}$ = 0.49, p = 0.039) when the foreground contrast was high and there was background interference [F100, B100]. When the foreground contrast was low, no correlation between θ and GABA+ was observed (Table 4).

In contrast, at placebo in the ASD group, also as predicted, there was no correlation between θ and GABA+ in any contrast condition - suggesting an uncoupling of the 'typical' relationship between GABA and SSVEP responses in conditions of high foreground and high background contrast.

Arbaclofen 'rescues' atypical visual processing in ASD and disrupts it in controls.

In ASD, the effect of foreground contrast on θ became significant following low dose arbaclofen (es = 0.14, p = 0.038), while the effect of background interference remained to be not significant (es = 0.13, p = 0.058). At high dose arbaclofen, however, the effect of both background and foreground contrast became significant (BI: es = -0.28, p = 3.88×10^{-6}; FC: es = 0.14, p = 0.012).

By contrast, arbaclofen had opposite effects on controls. The effects of both background interference and foreground contrast observed in controls at baseline remained significant at low dose condition (BI: es = -0.26, p = 2.18×10^{-4}; FC: es = 0.16, p = 0.021), but were disrupted to be not significant following high dose arbaclofen (BI: es = 0.13, p = 0.086; FC: es = 0.1, p = 0.165). ***Thus, in neurotypicals sensitivity to visual stimuli was disrupted by excess $GABA_B$ activation, whilst in ASD it was made more 'typical'.***

This drug effect was confirmed by the pair-wise SVM classification results. There was a significant difference between controls at placebo and high dose (ca = 78.5%, p = 0.013); and between autistic participants at placebo and high dose (ca = 73%, p = 0.038). As expected, the significant group difference (ca = 70.5%, p = 0.033) between controls and ASD at placebo was abolished by high dose arbaclofen – autistic participants given 30 mg arbaclofen could not be separated from controls taking placebo (ca = 52%, p = 0.442).

Post-hoc testing: Individual sensitivity and responsivity in ASD.

Given that drug treatment elicited a 'neurotypical' SSVEP response profile in the ASD group following high dose arbaclofen, we examined data from ASD participants who had completed both placebo and high-dose visits. For each visit, we calculated an individual 'sensitivity index' of visual processing profile across minimum and maximum stimulation configurations:

$$\Delta\theta = \theta[F100, B0] - \theta[F30, B100] \tag{3}$$

We confirmed that the shift in the sensitivity index $\Delta\theta$ elicited by 30mg arbaclofen was significant ($t_{(12)} = -5.14$, $p < 0.001$) within the ASD group using post-hoc paired t-test. In the high dose condition, 100% of the ASD group showed an increase in $\Delta\theta$ following 30 mg arbaclofen. Please see Fig. 6.

Discussion

Our results confirm that autistic participants have atypical GABA-dependent visual

processing. We demonstrate that these can be reversed by targeting $GABA_B$ receptors. An individual sensitivity index in ASD captured the change in visual processing in response to 30 mg arbaclofen. This has important implications for the development and testing of interventions which target fundamental sensory differences in ASD.

$GABA_B$ receptors are conventionally thought to provide tonic inhibition, however they can also rapidly inhibit neural network activity (*27*). The typical brain likely relies upon both mechanisms to fine tune neuronal processes. When $GABA_B$ activation is excessive, as in the 30 mg arbaclofen condition, this imbalance in GABAergic mechanisms alters responsivity to visual stimulation in neurotypicals. In contrast, increasing $GABA_B$ activity in ASD and elicits a more neurotypical response.

The reason(s) for this are unknown. Although post-mortem studies report fewer $GABA_B$ receptors in ASD (*38*), our findings cannot be explained simply by fewer $GABA_B$ receptors in ASD and compensation by arbaclofen. The effects observed in ASD occur at comparable concentrations of GABA in occipital cortex (though ^{1}H-MRS provides bulk tissue measures of metabolites, not synaptic concentration of neurotransmitters). Hence, even with fewer $GABA_B$ receptors, given adequate concentration of GABA to occupy available receptors, arbaclofen would have no or limited targets to act upon.

A more plausible explanation is that there is a difference in the functioning of $GABA_B$ receptor pathways in sensory circuits in ASD. Our study cannot establish what that difference may be, but $GABA_B$ receptors are modulatory and may exert a range of different cellular effects as they can act both pre- and post-synaptically to

alter cellular excitability (*39-42*). They also interact both with glutamate receptors (*43*) and $GABA_A$ receptors (*27, 28*) to influence neuronal signaling. Therefore, targeting $GABA_B$ receptor may alter a range of mechanisms which regulate E-I function. GABA (*12, 38*) and glutamate (*44, 45*) receptors families have been reported to be altered in ASD, as have the synapses which host these receptors (*46*), thus different response to $GABA_B$ receptor activation in people with and without ASD is likely to be underpinned by complex molecular differences in these cohorts.

Ultimately, the mechanism underpinning autistic sensory differences is likely to be complex, as $GABA_B$ activation has pre- and post-synaptic effects and can cause both inhibition and dis-inhibition (*47*). Autistic participants processed visual stimuli with equal salience regardless of their contrast, or background interference. There was no adaption to changing stimulus demands. High-dose arbaclofen elicited a neurotypical response in ASD, and sensitivity to changing stimulus demands. Thus, boosting $GABA_B$ may restore excitation-inhibition balance driving sensory perception. This fits with evidence that $GABA_B$ receptors support neuronal adaption to changes in activity levels (*47*).

Others have proposed computational models to help explain sensory processing in the typical and autistic brain. Using a motion perception task, Schallmo and colleagues recorded less neural suppression in ASD compared to neurotypicals, which they attributed to differences in top-down processing (*8*). In line with our findings and others (*16, 17, 21*), this group also found no differences in MR spectroscopy measurements of occipital GABA+ in ASD. However, unlike motion discrimination

that involves higher-order cognition, our paradigm was passive and did not rely on higher-order decision-making process. The neural mechanisms involved in these tasks are not exactly the same. While there may be a link between weaker spatial suppression in ASD (*8*), and the weaker suppression of background interference, no-one has directly manipulated GABA pathways in more complex tests of neural suppression in ASD.

Our findings do not speak to the clinical efficacy of arbaclofen – but may nevertheless have important implications for the development of interventions targeting core ASD symptomatology. In conventional ASD trials, primary outcome measures generally rely upon measures of sophisticated behaviours; for example, the Aberrant Behavior Checklist - Irritability; the Social Responsiveness Scale; the Vineland Adaptive Behavior Scale; and so on (*33, 34*). Such behaviours are highly complex, the product of multiple higher-order processes built upon lower-order processes and shaped by variable gene-environment interactions throughout life. An alternative approach may be to first establish if a candidate drug modifies a core neurobiological process (such as sensory processing) in ASD, and test efficacy in that domain (rather than more generally).

Our findings also do not speak to when differences in GABAergic processes arise in ASD, a neurodevelopmental condition with origins in very early life. Brain development is comprised of multiple, 'cascading' sensitive periods for different neural circuits/complex functions which continue throughout childhood and adolescence (*48*). Maturation of primary brain circuits, especially sensory circuits in

which GABA has a key role (*46, 49*), is a necessary foundation for higher-order processes. Thus, the atypical visual sensory processing observed here could be a consequence of an earlier disruption to neuronal circuit maturation. This concept is consistent with our recent work in newborn infants, where we found differences in the functional activity of visual sensory networks are already evident at birth in neonates with a higher likelihood of later receiving a diagnosis of ASD (*50*). Preclinical work using a mouse model with deletion of the autism-associated gene SHANK3 also supports altered homeostatic regulation in the early visual system (*51*). Early differences in the visual system however may not necessarily be impairing, and indeed enhanced visual search performance in infants with a higher likelihood of diagnosis of ASD has also been reported (*52*).

Our work cannot tell us whether atypical neurophysiological measures are related to perceptual differences in ASD. That is, this paradigm does not allow us to say whether $GABA_B$ receptor agonist would alter perception in either group, but a study of the impact of arbaclofen on perception would be of value. In this study, autistic participants had an essentially unchanging electrophysiological response to foreground stimuli regardless of contrast or background interference. Thus, there was both hypo-responsivity (in [F100, B0]) and hyper-responsivity (in [F30, B100]) in neural activities in the ASD group; all stimuli had equal salience. An unanswered question is whether stimuli processed uniformly in the visual cortex in ASD also gain indiscriminate access to higher order processing. If so, an ability to detect and respond to low contrast stimuli in conditions of high interference might sometimes be

advantageous and support the acquisition of particular skills; at other times it may lead to the sensory 'over-load' and distress often reported by autistic individuals.

Overwhelming sensory demands throughout life would understandably make it difficult to communicate with the world around us (*53*) and divert resources away from academic achievement (*54*), friendships and social life (*55*). Extreme sensitivity to particular types of light or flickering lights (*56*) might prevent an individual from performing basic daily living task, such as using medical facilities where light conditions may be distressing for autistic individuals (*57*). Moreover, indiscriminate processing of sensory stimuli has been suggested to allow repetitive sensory preferences and hence repetitive behavior to develop (*58*). Sensory processes are therefore fundamental to ASD and the current findings open new avenues to encourage examination of pharmacological interventions which specifically target the sensory domain in ASD, possibly through $GABA_B$ receptor. This has never been done before.

Limitations. We acknowledge the modest sample size in this study. In mitigation, the same participants returned for repeat visits thereby reducing heterogeneity and increasing power.

GABA+ comprises a mixture of neurotransmitter and metabolic pools (*59*), themselves in rapid exchange. Despite normal 'bulk' concentration of occipital cortical GABA+ we cannot rule out the possibility that synaptic concentration of GABA were altered in ASD. Also, GABA+ includes the contribution of

macromolecules (MM) (*36, 37*). It is unlikely that MM signal would be related to a neuronal processing and influence the associations observed.

Despite the passive nature of the task there were still some requirements for participation (e.g. wearing a recording cap and maintaining fixation on screen), potentially limiting the widest generalization across ages or to the broader autism spectrum. The absence of concurrent eye tracking made it hard to rule out the potential interference by unequal fixation between the control and ASD group, which should be carefully evaluated in future work. However, our hope is that this approach might be useful for at least some of the individuals with cognitive deficits and/or verbal communication difficulties that are frequently excluded from drug development studies.

There were also hardware constraints in the visual processing paradigm: We did not use the antiphase between upper and lower disks to attain higher SNR or stronger SSVEP (*32*), potentially impacting upon the power of our analyses. Similarly, we opted for a limited number of visual stimuli configurations; one low- and one high-contrast foreground conditions unlike previous paradigms (*30*). This reduced the range of SSVEP responses and might have limited the changes of observing a more fine-tuned effect; however, the shortest possible task was least burden to participants while still covering a range of meaningful effects.

Known side effects of arbaclofen (fatigue, dizziness, nausea) were reported throughout the study but were most evident at the high dose condition. 'Moderate' was defined by study team consensus as a relative term meaning more than 'mild'.

Mild side effects were very minimal – essentially any passing mention of side effects and less than 'severe' (not reported) and reflected a clear comment from the participant of a noticeable experience. This was not evaluated in terms of impact on function. The observed side effects could still potentially limit acute dose studies by impacting upon the participants' attentional resources allocation during the task. However, the attentional demand of this paradigm was small and limited to a short duration (about 6 minutes), and the participants were closely monitored by the researcher to ensure that the participant was comfortable and able to complete testing. Furthermore, an important issue for basic research in acute dose study designs, as well as trial design for evaluation of new or repurposed drugs for ASD and related conditions, is the dose regimen selected (*60-62*). In our study, acute drug effects on the SSVEPs were only evident at the higher dose (in both groups), therefore we would have 'missed' an effect if we had used the lower dose. However, the response to acute doses does not allow us to predict the dose needed for the long-term therapeutic response. In Clinical Trials there is usually titration and future studies should investigate how these acute responses relate to longer term drug administration.

Conclusion

We report direct pharmacological evidence that differences in GABA pathways are responsible for visual processing anomalies in people with ASD; and these differences can be abolished by (high dose) $GABA_B$ receptor activation. We cannot say if our results will generalize to different developmental stages (e.g. children) or to

the broader autism spectrum, namely those with learning disabilities, however we hope that this short, passive task will be of use for individuals often precluded from drug development studies. Passive testing means we need not rely upon assumptions that participants understand interpret and/or perform the task in the same way. This accessible proxy marker for individual GABAergic differences can be 'shifted' by a candidate medication. This may help identify more biologically homogeneous subgroups of individuals and so underpin efforts to develop more 'personalized medicine' approaches in ASD.

Materials and Methods

Study design. In this double-blind, placebo-controlled, cross-over experiment, 44 participants (25 controls, 19 ASD) were given a single oral dose of 15 mg or 30 mg arbaclofen (STX209) or placebo on the study day, 1 hour before ^{1}H-MRS and 3 hours before the EEG visual testing. Ninety-four study visits were completed and the order was randomized across visits. Arbaclofen plasma concentration are expected to peak at 1 hour after intake and have a half-life of 5 hours (*63*), thus EEG testing was within the active physiological window. Neither researchers nor participants knew whether a placebo or active drug was administered on visits.

Medical cover was provided throughout each test session and participants were asked to remain at our unit until at least 4 hours post drug/placebo administration. The medic was 'blind' to the order of administration but had access to the randomization codes held at our pharmacy and by the Chief Investigator in the event that emergency

code break was required. No emergency code break was required, but where a participant had experienced side-effects which were more than moderate in the opinion of the study medic and after discussion with the Chief Investigator, unblinding occurred to try to avoid exposure to a higher dose of arbaclofen on a subsequent visit.

Participants. For the ASD group, approximately 50% of participants (9/19) were recruited from our National Autism and ADHD Service for Adults (NAASA) at the South London and Maudsley NHS Foundation Trust, a national specialist NHS referral center for adults with autism; the service protocol includes an Autism Diagnostic Interview-Revised (ADI-R) (*64*) where an appropriate informant is available and/or Autism Diagnostic Observation Schedule (ADOS) (*65*) to inform the assessment and/or current symptom level respectively: (https://www.slam.nhs.uk/national-services/adult-services/adhd-and-asd-services-outp atients/). Other potential participants were carefully screened by an experienced clinician from NAASA who was satisfied by the account of their diagnostic assessment through a recognised U.K. autism service. ASD traits were also assessed across both the control group and the ASD group using the Autism Quotient (AQ; (*66*)). As expected, there was a highly significant group difference in AQ ($t_{(41)} = 8.9$, p $= 3.78 \times 10^{-11}$); please see Table 5.

Demographic characteristics including biological sex and intelligence quotient (IQ; on the Wechsler Abbreviated Scale of Intelligence; WASI-II (*67*)) did not differ

between the two participant groups (Table 5). All participants were adults. The age range of ASD and control groups was similar (19-51 years and 19-52 years respectively), although the mean age of the ASD group (37.3 years) was higher than that of the control group (30.4 years) ($t_{(44)}$ = 2.39, p = 0.022). However, there was no relationship between any electrophysiological measures and age in either group, thus age differences were unlikely to explain any group differences reported. Autistic participants caused by a known genetic syndrome, such as fragile X syndrome or 22q11 deletion syndrome, were excluded from the study.

Other inclusion criteria were as follows: IQ>70, normal or correct-to-normal sight, ability to give informed consent, no comorbid psychiatric illness (e.g., psychotic illness and major mood disorder), no history of seizures or diagnosis of epilepsy, and no physical illness, such as heart disease, high blood pressure and renal insufficiency. In the month preceding participation, thirteen participants (5 controls, 8 ASD) were taking regular medication with drugs such as ibuprofen, paracetamol and sertraline, which did not affect glutamate or GABA directly. All other participants were medication free.

As expected, recruitment of autistic males was faster than autistic females, therefore we completed testing of male participants before female participants. Where a participant complained of side-effects following administration of the study drug, we unblinded after testing. This way, if they had received the low dose of arbaclofen we could cancel their high dose visit and avoid further discomfort. We noted that controls were somewhat more likely to experience the known side-effects of

arbaclofen (especially nausea and dizziness), particularly when given the high dose. When this pattern continued with control females, we discussed with the ethics committee and re-ordered the blinded administration order such that low dose arbaclofen always preceded high dose for the remaining females (both ASD and controls). This way, if a participant experienced uncomfortable side-effects we could unblind for that visit and cancel the high dose visit if appropriate. We had to do this for 1 control and 1 ASD participant. Of the 30 participants who received 15 mg arbaclofen, 9 (5 ASD, 4 controls) reported known side effects such as fatigue, dizziness and nausea; of the 26 (14 ASD, 12 controls) participants who received 30 mg arbaclofen, 18 (9 ASD, 9 controls) reported these side effects as at least moderate.

^{1}H-MRS data acquisition. Participants were scanned on a GE Discovery MR750 3T scanner (Milwaukee, WI, USA) using a 12-channel birdcage head coil at the Centre for Neuroimaging Sciences, King's College London. A 3D T_1-weighted high resolution anatomical scan using the protocol developed by the Alzheimer's Disease Neuroimaging Initiative (ADNI-GO) sagittal Inversion-Recovery Fast Spoiled Gradient Recalled (IR-FSPGR) with repetition time (TR) = 7.312 ms, echo time (TE) = 3.016 ms, inversion time (TI) = 400 ms, flip angle (FA) 11°, field of view 270 mm, 256 × 256 × 196 matrix, voxel dimensions (left-right (LR), anterior-posterior (AP),superior-inferior (SI):): 1.055 x 1.055 x 1.2 mm was acquired for each participant. This T_1-weighted anatomical scan was then used to prescribe the ^{1}H-MRS voxel and later for voxel tissue segmentation for further metabolite tissue corrected

quantification.

The HERMES implementation used is a double experiment designed to edit both the GABA and the glutathione signal (*35*). Since only the GABA signal is relevant for the current work, we report sequence parameters and metabolite quantification methods relevant for the GABA experiment only. HERMES parameters were: TR = 2 s, TE = 80 ms, 352 averages: 176 ON and 176 OFF, 4096 data points, bandwidth 5 kHz, phase cycle length of 2, 90° excitation pulses, 137° slice-selective refocusing pulses and 180° sinc-Gaussian editing pulses with 20 ms duration applied at 1.9 ppm in the ON averages and at 7.22 ppm in the OFF averages. Chemical Shift Selective (CHESS) water suppression was used. Auto pre-scan was run twice to ensure water linewidth < 9 Hz before starting the scan. Finally, 16 unsuppressed water scans with the same parameters were also acquired for further water-scaling metabolite quantification and eddy-current correction. The voxel was prescribed in the medial occipital cortex along the brain midline and parallel to the tentorium mostly comprising the visual areas pericalcarine, cuneus, precuneus and lingual gyrus [dimensions LR: 30 mm; AP: 30 mm; SI: 25 mm; 22.5 mL]. Total ^{1}H-MRS scan duration was approximately 13 minutes.

The majority (10 ASD, 13 controls) completed ^{1}H-MRS and EEG visual testing on the same visit day; with the visual testing following scanning and approximately 3 hours after drug/placebo administration. Where this was not possible, the remaining participants completed the visual testing on a separate day without scanning; the timing of data acquisition post drug/placebo administration was comparable

regardless of whether participants completed scanning and visual testing on the same or on separate days.

Metabolite qualification. Raw ^{1}H-MRS spectra were pre-processed using in-house scripts adapted from FID appliance (FID-A pre-processing pipeline (*68*) (www.github.com/CIC-methods/FID-A) running in MATLAB. FID-A pre-processing steps included weighted receiver coil combination, removal of motion corrupted averages, frequency and phase drift correction, and spectral registration to align ON and OFF sub-spectra, prior to subtraction to minimize subtraction artifacts (*69*). The outputs of FID-A include the GABA difference spectrum and the unsuppressed water signal (used for eddy-current correction and water-scaled metabolite quantification). These files were then fed into LCModel v 6.3-1L (Stephen Provencher Inc., Oakville, Canada) for GABA+ quantification from the GABA difference spectra (Supplementary Fig. S2). All spectra were visually inspected to ensure only good quality data were included in the analysis. The ^{1}H-MRS voxel was segmented to extract the proportion of gray matter, white and cerebrospinal fluid for further metabolite tissue correction. Please see Supplementary Materials (Table S1 and Table S2) for statistical and subject-level details on metabolite quantification, data quality and voxel tissue composition.

Visual paradigm. Visual stimuli were created in MATLAB using the Psychophysics Toolbox (*70*). Our visual contrast sensitivity paradigm consisted of two parts: (i) four

flickering circular foreground gratings with sinusoidal vertical Gabor grating patterns (1 cycle/degree, radius of 2°); (ii) the rest of the screen formed the static background. Foreground gratings were placed around the center of the screen with an eccentricity of 4° of visual angle, which were designed to stimulate the peripheral receptive field. The polar angles of the two upper/lower gratings were 45°/20°, respectively, referenced to the horizontal meridian crossing the central point. This asymmetrical setting was consistent with previous studies on the polarity of visual evoked potentials to stimulate both the upper and lower banks of the calcarine fissure (*71-73*).

Testing was conducted in a darkened room at the Sackler Institute for Translational Neurodevelopment, King's College London. The participant was comfortably seated and leaned on a chin rest, viewing the monitor at 60 cm. The test consisted of 60 stimulation trials, in which the stimuli were pseudorandomly presented 10 times under each of the six stimulus configurations: [F0, B0], [F30, B0], [F100, B0], [F0, B100], [F30, B100] and [F100, B100]. As a trial began, a static cross was presented at the center of the screen. The participant was instructed to passively stare at the cross throughout the trial and blink normally. After 500 ms (the inter trial interval), the foreground gratings synchronously performing on-off flickering at 20 Hz were presented for 2.9 s, to elicit SSVEP components in EEG at the flickering frequency as well as its harmonic waves. After every 10 trials, a 6-s break was provided for the participant to relax.

Scalp EEG signals were collected using a 64-channel standard actiCAP (EASYCAP GmbH, Herrsching, Germany) with a sampling rate of 5 KHz and

amplified by a BrainAmp amplifier (Brain Products GmbH, Gilching, Germany). Electrode placements followed the international 10-20 system (*74*). Impedances between the scalp and electrodes were kept below 15 kΩ.

EEG data processing. On each participant visit, we extracted an EEG epoch for each stimulation trial in the interval [-500, 2900] ms referenced to the flickering onset at 0 ms. The baseline was corrected by subtracting the mean value of the interval [-200, 0] ms. Next, all EEG epochs were down-sampled to 250 Hz and filtered by a bandpass filter with [3, 45] Hz. Epochs that maintained a peak value over 40 μV were regarded as contaminated by eye blinks or unexpected movements and excluded from further analysis. The filtered EEG epochs were then averaged by the six stimulus configurations. Finally, a subset of each averaged epoch in the interval [160, 2900] ms was extracted and reserved for further analysis. The 160-ms delay was an approximation of the SSVEP response time.

We measured elicited SSVEP components in the pre-processed EEG epochs using canonical correlation analysis (CCA). CCA evaluates the underlying correlation between two multidimensional variables and has been increasingly applied to detect SSVEPs (*75*). For each stimulus configuration, the pre-processed EEG epoch was a multichannel variable $X = (x_1, x_2, ..., x_m)$, where m = 6 was the number of selected channels, and x_i represented the sample vector of the i th channel. Given a group of template signals $Y = (y_1, y_2, ..., y_n)$, the goal of the CCA was to find two weight vectors ω_X and ω_Y that maximized the correlation coefficient between the linear

transformations $U = \omega_X^T X$ and $V = \omega_Y^T Y$ by solving the following problem:

$$\max \rho(U,V) = \frac{\omega_X^T \operatorname{cov}(X,Y)\omega_Y}{\sqrt{\omega_X^T \operatorname{cov}(X,X)\omega_X}\sqrt{\omega_Y^T \operatorname{cov}(Y,Y)\omega_Y}} \tag{4}$$

where ρ was the correlation coefficient, $\operatorname{cov}(X,Y)$ represented the cross-covariance matrix of X and Y, whose (i,j) entry was the covariance $\operatorname{cov}(x_i, y_j)$. In this study, the template Y was set to be a group of sinusoid signals:

$$Y = \begin{bmatrix} \sin(2\pi ft) \\ \cos(2\pi ft) \\ \sin(4\pi ft) \\ \cos(4\pi ft) \end{bmatrix}^T \tag{5}$$

where f was the template frequency, which approximated the stimulus frequency. Since the template Y was used to simulate the ideal SSVEP oscillation, a higher ρ meant that the elicited SSVEP was more prominent.

Since the foreground gratings did not flash when contrast was 0% (F0), the coefficient ρ of configuration [F0, B0] and [F0, B100] were used as baselines to further reduce the effect of individual differences by calculating a relative SSVEP increase θ as follows:

$$\begin{cases} with\_BI : \theta[Fi, B100] = \dfrac{\rho[Fi, B100] - \rho[F0, B100]}{\rho[F0, B100]} \\ no\_BI : \theta[Fi, B0] = \dfrac{\rho[Fi, B0] - \rho[F0, B0]}{\rho[F0, B0]} \end{cases} \tag{6}$$

where BI was the background interference, i was the absolute value of the non-zero foreground contrast, which could be 30 or 100. Please see Supplementary Materials (Table S3) for subject-level θ values for the six participant groups.

Statistical analysis. Independent-sample t test was used to assess group differences of

occipital GABA+ concentration and surround suppression (SS) values at placebo, and was corrected for multiple comparisons using Benjamini-Hochberg method (*76*). Then, we ran a 2 x 3 split-plot ANOVA for occipital GABA+ concentration with group (ASD, control) as between-subject factor and drug (placebo, low-dose and high-dose) as within-subject factor. A correlation analysis was performed between occipital GABA+ concentration and the extracted EEG features, i.e. the θ values. Reported *r* values are Pearson's linear correlation coefficients; associated *p* values were computed using a Student's t distribution for a transformation of the correlation.

Statistical analysis of the θ values performed using LMM. To investigate how the fixed effects of foreground contrast and background interference on θ were modulated by the drug dose in either controls or ASD participants, we built a LMM model of the θ value (response factor) for each of the six participant groups, in which the foreground contrast and background interference were set as fixed effect factors, gender as covariate, and subject was the random effect factor. Please see Supplementary Materials – EEG data processing section for more LMM results of interaction effects. Moreover, to probe whether at placebo SSVEP responses in controls and ASD participants during background interference were related to occipital GABA+, we calculated the correlation coefficients between the placebo θ during background interference and the corrected metabolite value Met_{corr}.

We also applied an SVM method to further investigate whether there was a difference in the overall pattern of SSVEP responses across all conditions between the six participant groups. In this study, the extracted 4-d θ feature vector was used as

input for SVM model training as it contained dynamic information of SSVEP responses in that participant visit. We trained an SVM model to classify between each pair of the 6 groups. For example, to measure how the overall response of Control_P was different from that of ASD_P, we first balanced the feature vector sets of Control_P and ASD_P by random oversampling. Next, following a 10-fold cross validation pipeline, θ feature vectors from the two groups were labelled differently (e.g., labeled Control_P as '1' and ASD_P as '-1') and fed into the SVM classifier training and testing processes. The 10-fold cross validation process was then repeated 10 times, and the average accuracy ca was recorded.

Statistical significance of ca was determined using permutation testing. Specifically, we merged θ feature vectors from the two groups and then pseudorandomly labelled them into two balanced sets. An average accuracy could be obtained following a repeated 10-fold cross validation process. This permutation procedure was then repeated 10,000 times to achieve an accuracy set $[ca_i]$, which approximated the true distribution. The p value associated with ca was defined as the probability that a random sample from $[ca_i]$ was larger than or equal to ca, and was corrected using MaxT procedure (77). Thus, if $p < 0.05$, we could say that ca was significantly higher than random, and the dynamic SSVEP responses of the two participant groups were therefore different.

Supplementary Materials

Materials and Methods

Fig. S1. Medial occipital GABA+ concentrations for both groups at all experimental conditions.

Fig. S2. Medial occipital GABA+ representative spectrum.

Table S1. 1H-MRS data quality indicators and voxel tissue composition for the two groups with corresponding between-group comparisons for the GABA-difference spectra.

Table S2. ^{1}H-MRS GABA+ concentration, spectra quality metrics, and voxel tissue proportion for both groups at each drug condition.

Table S3. The SSVEP value θ at different stimulus conditions for both groups at each drug condition.

Reference (*78-90*)

References

1.	A. P. Assoc, Diagnostic and statistical manual of mental disorders. *Edition, Fifth*, (2013).
2.	S. Dakin, U. Frith, Vagaries of visual perception in autism. *Neuron* **48**, 497-507 (2005).
3.	D. R. Simmons, A. E. Robertson, L. S. McKay, E. Toal, P. McAleer, F. E. Pollick, Vision in autism spectrum disorders. *Vision research* **49**, 2705-2739 (2009).
4.	C. E. Robertson, D. J. Kravitz, J. Freyberg, S. Baron-Cohen, C. I. Baker, Slower rate of binocular rivalry in autism. *Journal of Neuroscience* **33**, 16983-16991 (2013).
5.	J. H. Foss-Feig, D. Tadin, K. B. Schauder, C. J. Cascio, A substantial and unexpected enhancement of motion perception in autism. *Journal of Neuroscience* **33**, 8243-8249 (2013).
6.	C. E. Robertson, C. Thomas, D. J. Kravitz, G. L. Wallace, S. Baron-Cohen, A. Martin, C. I. Baker, Global motion perception deficits in autism are reflected as early as primary visual cortex. *Brain* **137**, 2588-2599 (2014).
7.	J. Horder, M. Andersson, M. A. Mendez, N. Singh, Ä. Tangen, J. Lundberg, A. Gee, C. Halldin, M. Veronese, S. Bölte, GABAA receptor availability is not altered in adults with autism spectrum disorder or in mouse models. *Science translational medicine* **10**, (2018).
8.	M.-P. Schallmo, T. Kolodny, A. M. Kale, R. Millin, A. V. Flevaris, R. A. Edden, J. Gerdts, R. A. Bernier, S. O. Murray, Weaker neural suppression in autism. *Nature communications* **11**, 1-13 (2020).
9.	J. Rubenstein, M. M. Merzenich, Model of autism: increased ratio of excitation/inhibition in key neural systems. *Genes, Brain and Behavior* **2**, 255-267 (2003).
10.	O. Yizhar, L. E. Fenno, M. Prigge, F. Schneider, T. J. Davidson, D. J. O'shea, V. S. Sohal, I. Goshen, J. Finkelstein, J. T. Paz, Neocortical excitation/inhibition balance in information processing and social dysfunction. *Nature* **477**, 171-178 (2011).
11.	J. H. Foss-Feig, B. D. Adkinson, J. L. Ji, G. Yang, V. H. Srihari, J. C. McPartland, J. H. Krystal, J. D. Murray, A. Anticevic, Searching for cross-diagnostic convergence: neural mechanisms governing excitation and inhibition balance in schizophrenia and autism spectrum disorders. *Biological psychiatry* **81**, 848-861 (2017).
12.	S. H. Fatemi, T. J. Reutiman, T. D. Folsom, P. D. Thuras, GABA A receptor downregulation in brains of subjects with autism. *Journal of autism and developmental disorders* **39**, 223 (2009).
13.	H.-T. Chao, H. Chen, R. C. Samaco, M. Xue, M. Chahrour, J. Yoo, J. L. Neul, S. Gong, H.-C. Lu, N. Heintz, Dysfunction in GABA signalling mediates autism-like stereotypies and Rett syndrome phenotypes. *Nature* **468**, 263-269 (2010).
14.	R. Pizzarelli, E. Cherubini, Alterations of GABAergic signaling in autism spectrum disorders. *Neural plasticity* **2011**, (2011).
15.	S. Han, C. Tai, R. E. Westenbroek, H. Y. Frank, C. S. Cheah, G. B. Potter, J. L. Rubenstein, T. Scheuer, O. Horacio, W. A. Catterall, Autistic-like behaviour in Scn1a+/− mice and rescue by enhanced GABA-mediated neurotransmission. *Nature* **489**, 385-390 (2012).
16.	N. A. Puts, E. L. Wodka, A. D. Harris, D. Crocetti, M. Tommerdahl, S. H. Mostofsky, R. A. Edden, Reduced GABA and altered somatosensory function in children with autism spectrum disorder. *Autism Research* **10**, 608-619 (2017).
17.	W. Gaetz, L. Bloy, D. Wang, R. G. Port, L. Blaskey, S. Levy, T. P. Roberts, GABA estimation in the brains of children on the autism spectrum: measurement precision and regional cortical

variation. *Neuroimage* **86**, 1-9 (2014).

18. G. S. Drenthen, E. M. Barendse, A. P. Aldenkamp, T. M. van Veenendaal, N. A. Puts, R. A. Edden, S. Zinger, G. Thoonen, M. P. Hendriks, R. P. Kessels, Altered neurotransmitter metabolism in adolescents with high-functioning autism. *Psychiatry Research: Neuroimaging* **256**, 44-49 (2016).

19. D. A. Edmondson, P. Xia, R. McNally Keehn, U. Dydak, B. Keehn, A Magnetic Resonance Spectroscopy Study of Superior Visual Search Abilities in Children with Autism Spectrum Disorder. *Autism Research* **13**, 550-562 (2020).

20. T. Kolodny, M. P. Schallmo, J. Gerdts, R. A. Edden, R. A. Bernier, S. O. Murray, Concentrations of cortical GABA and glutamate in young adults with autism spectrum disorder. *Autism Research*, (2020).

21. C. E. Robertson, E.-M. Ratai, N. Kanwisher, Reduced GABAergic action in the autistic brain. *Current Biology* **26**, 80-85 (2016).

22. R. G. Port, W. Gaetz, L. Bloy, D. J. Wang, L. Blaskey, E. S. Kuschner, S. E. Levy, E. S. Brodkin, T. P. Roberts, Exploring the relationship between cortical GABA concentrations, auditory gamma‐band responses and development in ASD: Evidence for an altered maturational trajectory in ASD. *Autism Research* **10**, 593-607 (2017).

23. Q. Chen, C. A. Deister, X. Gao, B. Guo, T. Lynn-Jones, N. Chen, M. F. Wells, R. Liu, M. J. Goard, J. Dimidschstein, Dysfunction of cortical GABAergic neurons leads to sensory hyper-reactivity in a Shank3 mouse model of ASD. *Nature neuroscience* **23**, 520-532 (2020).

24. D. C. Rojas, D. Singel, S. Steinmetz, S. Hepburn, M. S. Brown, Decreased left perisylvian GABA concentration in children with autism and unaffected siblings. *Neuroimage* **86**, 28-34 (2014).

25. C. E. Robertson, S. Baron-Cohen, Sensory perception in autism. *Nature Reviews Neuroscience* **18**, 671 (2017).

26. M. Farrant, Z. Nusser, Variations on an inhibitory theme: phasic and tonic activation of GABA A receptors. *Nature Reviews Neuroscience* **6**, 215-229 (2005).

27. M. T. Craig, C. J. McBain, The emerging role of GABAB receptors as regulators of network dynamics: fast actions from a 'slow'receptor? *Current opinion in neurobiology* **26**, 15-21 (2014).

28. W. M. Connelly, S. J. Fyson, A. C. Errington, C. P. McCafferty, D. W. Cope, G. Di Giovanni, V. Crunelli, GABAB receptors regulate extrasynaptic GABAA receptors. *Journal of Neuroscience* **33**, 3780-3785 (2013).

29. J. Mentch, A. Spiegel, C. Ricciardi, C. E. Robertson, GABAergic inhibition gates perceptual awareness during binocular rivalry. *Journal of Neuroscience* **39**, 8398-8407 (2019).

30. N. Langer, E. J. Ho, L. M. Alexander, H. Y. Xu, R. K. Jozanovic, S. Henin, A. Petroni, S. Cohen, E. T. Marcelle, L. C. Parra, A resource for assessing information processing in the developing brain using EEG and eye tracking. *Scientific data* **4**, 1-20 (2017).

31. T. Z. Lauritzen, J. M. Ales, A. R. Wade, The effects of visuospatial attention measured across visual cortex using source-imaged, steady-state EEG. *Journal of vision* **10**, 39-39 (2010).

32. M. I. Vanegas, A. Blangero, S. P. Kelly, Electrophysiological indices of surround suppression in humans. *Journal of neurophysiology* **113**, 1100-1109 (2015).

33. C. A. Erickson, J. M. Veenstra-Vanderweele, R. D. Melmed, J. T. McCracken, L. D. Ginsberg, L. Sikich, L. Scahill, M. Cherubini, P. Zarevics, K. Walton-Bowen, STX209 (arbaclofen) for autism spectrum disorders: an 8-week open-label study. *Journal of autism and developmental*

disorders **44**, 958-964 (2014).

34. J. Veenstra-VanderWeele, E. H. Cook, B. H. King, P. Zarevics, M. Cherubini, K. Walton-Bowen, M. F. Bear, P. P. Wang, R. L. Carpenter, Arbaclofen in children and adolescents with autism spectrum disorder: a randomized, controlled, phase 2 trial. *Neuropsychopharmacology* **42**, 1390-1398 (2017).

35. M. G. Saleh, G. Oeltzschner, K. L. Chan, N. A. Puts, M. Mikkelsen, M. Schär, A. D. Harris, R. A. Edden, Simultaneous edited MRS of GABA and glutathione. *Neuroimage* **142**, 576-582 (2016).

36. P. G. Henry, C. Dautry, P. Hantraye, G. Bloch, Brain GABA editing without macromolecule contamination. *Magnetic Resonance in Medicine: An Official Journal of the International Society for Magnetic Resonance in Medicine* **45**, 517-520 (2001).

37. P. G. Mullins, D. J. McGonigle, R. L. O'Gorman, N. A. Puts, R. Vidyasagar, C. J. Evans, R. A. Edden, Current practice in the use of MEGA-PRESS spectroscopy for the detection of GABA. *Neuroimage* **86**, 43-52 (2014).

38. A. L. Oblak, T. T. Gibbs, G. J. Blatt, Decreased GABAB receptors in the cingulate cortex and fusiform gyrus in autism. *Journal of neurochemistry* **114**, 1414-1423 (2010).

39. G. Bonanna, A. Fassio, G. Schmid, P. Severi, R. Sala, M. Raiteri, Pharmacologically distinct GABAB receptors that mediate inhibition of GABA and glutamate release in human neocortex. *British journal of pharmacology* **120**, 60-64 (1997).

40. M. Gassmann, B. Bettler, Regulation of neuronal GABA B receptor functions by subunit composition. *Nature Reviews Neuroscience* **13**, 380-394 (2012).

41. M. S. Perkinton, T. S. Sihra, Presynaptic GABAB receptor modulation of glutamate exocytosis from rat cerebrocortical nerve terminals: receptor decoupling by protein kinase C. *Journal of neurochemistry* **70**, 1513-1522 (1998).

42. S. E. Thompson, G. Ayman, G. L. Woodhall, R. S. Jones, Depression of glutamate and GABA release by presynaptic GABAB receptors in the entorhinal cortex in normal and chronically epileptic rats. *Neurosignals* **15**, 202-215 (2006).

43. S. Kantamneni, Cross-talk and regulation between glutamate and GABAB receptors. *Frontiers in cellular neuroscience* **9**, 135 (2015).

44. A. Purcell, O. Jeon, A. Zimmerman, M. E. Blue, J. Pevsner, Postmortem brain abnormalities of the glutamate neurotransmitter system in autism. *Neurology* **57**, 1618-1628 (2001).

45. S. H. Fatemi, D. F. Wong, J. R. Brašić, H. Kuwabara, A. Mathur, T. D. Folsom, S. Jacob, G. M. Realmuto, J. V. Pardo, S. Lee, Metabotropic glutamate receptor 5 tracer [18 F]-FPEB displays increased binding potential in postcentral gyrus and cerebellum of male individuals with autism: a pilot PET study. *Cerebellum & ataxias* **5**, 1-8 (2018).

46. S. B. Nelson, V. Valakh, Excitatory/inhibitory balance and circuit homeostasis in autism spectrum disorders. *Neuron* **87**, 684-698 (2015).

47. F. H. Marshall, in *Inhibitory Regulation of Excitatory Neurotransmission*. (Springer, 2007), pp. 87-98.

48. J. Ciarrusta, R. Dimitrova, G. McAlonan, Early maturation of the social brain: How brain development provides a platform for the acquisition of social-cognitive competence. *Progress in Brain Research* **254**, 49-70 (2020).

49. N. Gogolla, A. E. Takesian, G. Feng, M. Fagiolini, T. K. Hensch, Sensory integration in mouse insular cortex reflects GABA circuit maturation. *Neuron* **83**, 894-905 (2014).

50.   J. Ciarrusta, R. Dimitrova, D. Batalle, J. O'Muircheartaigh, L. Cordero-Grande, A. Price, E. Hughes, J. Kangas, E. Perry, A. Javed, Emerging functional connectivity differences in newborn infants vulnerable to autism spectrum disorders. *Translational psychiatry* **10**, 1-10 (2020).

51.   V. Tatavarty, A. T. Pacheco, C. G. Kuhnle, H. Lin, P. Koundinya, N. J. Miska, K. B. Hengen, F. F. Wagner, S. D. Van Hooser, G. G. Turrigiano, Autism-associated Shank3 is essential for homeostatic compensation in rodent V1. *Neuron* **106**, 769-777. e764 (2020).

52.   T. Gliga, R. Bedford, T. Charman, M. H. Johnson, S. Baron-Cohen, P. Bolton, C. Cheung, K. Davies, M. Liew, J. Fernandes, Enhanced visual search in infancy predicts emerging autism symptoms. *Current Biology* **25**, 1727-1730 (2015).

53.   C. L. Hilton, J. D. Harper, R. H. Kueker, A. R. Lang, A. M. Abbacchi, A. Todorov, P. D. LaVesser, Sensory responsiveness as a predictor of social severity in children with high functioning autism spectrum disorders. *Journal of autism and developmental disorders* **40**, 937-945 (2010).

54.   F. E. Howe, S. D. Stagg, How sensory experiences affect adolescents with an autistic spectrum condition within the classroom. *Journal of autism and developmental disorders* **46**, 1656-1668 (2016).

55.   M. D. Thye, H. M. Bednarz, A. J. Herringshaw, E. B. Sartin, R. K. Kana, The impact of atypical sensory processing on social impairments in autism spectrum disorder. *Developmental Cognitive Neuroscience* **29**, 151-167 (2018).

56.   O. Bogdashina, *Sensory perceptual issues in autism and asperger syndrome: different sensory experiences-different perceptual worlds.*   (Jessica Kingsley Publishers, 2016).

57.   E. Giarelli, R. Nocera, R. Turchi, T. L. Hardie, R. Pagano, C. Yuan, Sensory stimuli as obstacles to emergency care for children with autism spectrum disorder. *Advanced Emergency Nursing Journal* **36**, 145-163 (2014).

58.   B. A. Boyd, M. McBee, T. Holtzclaw, G. T. Baranek, J. W. Bodfish, Relationships among repetitive behaviors, sensory features, and executive functions in high functioning autism. *Research in autism spectrum disorders* **3**, 959-966 (2009).

59.   C. D. Rae, A guide to the metabolic pathways and function of metabolites observed in human brain 1 H magnetic resonance spectra. *Neurochemical research* **39**, 1-36 (2014).

60.   J. L. Silverman, M. Pride, J. Hayes, K. Puhger, H. Butler-Struben, S. Baker, J. Crawley, GABA B receptor agonist R-baclofen reverses social deficits and reduces repetitive behavior in Two mouse models of autism. *Neuropsychopharmacology* **40**, 2228-2239 (2015).

61.   E. Berry-Kravis, R. Hagerman, J. Visootsak, D. Budimirovic, W. E. Kaufmann, M. Cherubini, P. Zarevics, K. Walton-Bowen, P. Wang, M. F. Bear, Arbaclofen in fragile X syndrome: results of phase 3 trials. *Journal of Neurodevelopmental Disorders* **9**, 1-18 (2017).

62.   O. D. Howes, M. Rogdaki, J. L. Findon, R. H. Wichers, T. Charman, B. H. King, E. Loth, G. M. McAlonan, J. T. McCracken, J. R. Parr, Autism spectrum disorder: Consensus guidelines on assessment, treatment and research from the British Association for Psychopharmacology. *Journal of Psychopharmacology* **32**, 3-29 (2018).

63.   R. Sanchez-Ponce, L.-Q. Wang, W. Lu, J. Von Hehn, M. Cherubini, R. Rush, Metabolic and pharmacokinetic differentiation of STX209 and racemic baclofen in humans. *Metabolites* **2**, 596-613 (2012).

64.   C. Lord, M. Rutter, A. Le Couteur, Autism Diagnostic Interview-Revised: a revised version of a

diagnostic interview for caregivers of individuals with possible pervasive developmental disorders. *Journal of autism and developmental disorders* **24**, 659-685 (1994).

65.   C. Lord, S. Risi, L. Lambrecht, E. H. Cook, B. L. Leventhal, P. C. DiLavore, A. Pickles, M. Rutter, The Autism Diagnostic Observation Schedule—Generic: A standard measure of social and communication deficits associated with the spectrum of autism. *Journal of autism and developmental disorders* **30**, 205-223 (2000).

66.   S. Baron-Cohen, S. Wheelwright, R. Skinner, J. Martin, E. Clubley, The autism-spectrum quotient (AQ): Evidence from asperger syndrome/high-functioning autism, malesand females, scientists and mathematicians. *Journal of autism and developmental disorders* **31**, 5-17 (2001).

67.   D. Wechsler, Wechsler Abbreviated Scale of Intelligence Second Edition (WASI-II) San Antonio. *TX: Pearson.[Google Scholar]*,   (2011).

68.   R. Simpson, G. A. Devenyi, P. Jezzard, T. J. Hennessy, J. Near, Advanced processing and simulation of MRS data using the FID appliance (FID‐A)—an open source, MATLAB‐based toolkit. *Magnetic resonance in medicine* **77**, 23-33 (2017).

69.   J. Near, R. Edden, C. J. Evans, R. Paquin, A. Harris, P. Jezzard, Frequency and phase drift correction of magnetic resonance spectroscopy data by spectral registration in the time domain. *Magnetic Resonance in Medicine* **73**, 44-50 (2015).

70.   D. H. Brainard, The psychophysics toolbox. *Spatial vision* **10**, 433-436 (1997).

71.   V. P. Clark, S. Fan, S. A. Hillyard, Identification of early visual evoked potential generators by retinotopic and topographic analyses. *Human brain mapping* **2**, 170-187 (1994).

72.   F. Di Russo, S. Pitzalis, G. Spitoni, T. Aprile, F. Patria, D. Spinelli, S. A. Hillyard, Identification of the neural sources of the pattern-reversal VEP. *Neuroimage* **24**, 874-886 (2005).

73.   M. I. Vanegas, A. Blangero, S. P. Kelly, Exploiting individual primary visual cortex geometry to boost steady state visual evoked potentials. *Journal of neural engineering* **10**, 036003 (2013).

74.   H. H. Jasper, The ten-twenty electrode system of the International Federation. *Electroencephalogr. Clin. Neurophysiol.* **10**, 370-375 (1958).

75.   X. Chen, Y. Wang, M. Nakanishi, X. Gao, T.-P. Jung, S. Gao, High-speed spelling with a noninvasive brain–computer interface. *Proceedings of the national academy of sciences* **112**, E6058-E6067 (2015).

76.   Y. Benjamini, Y. Hochberg, Controlling the false discovery rate: a practical and powerful approach to multiple testing. *Journal of the Royal statistical society: series B (Methodological)* **57**, 289-300 (1995).

77.   P. H. Westfall, S. S. Young, *Resampling-based multiple testing: Examples and methods for p-value adjustment*.   (John Wiley & Sons, 1993), vol. 279.

78.   S. W. Provencher, Automatic quantitation of localized in vivo 1H spectra with LCModel. *NMR in Biomedicine: An International Journal Devoted to the Development and Application of Magnetic Resonance In Vivo* **14**, 260-264 (2001).

79.   S. W. Provencher, Estimation of metabolite concentrations from localized in vivo proton NMR spectra. *Magnetic resonance in medicine* **30**, 672-679 (1993).

80.   Y. Zhang, L. An, J. Shen, Fast computation of full density matrix of multispin systems for spatially localized in vivo magnetic resonance spectroscopy. *Medical physics* **44**, 4169-4178 (2017).

81.   D. Rotaru, D. Lythgoe, in *Proceedings of the 26th Annual Meeting of the ISMRM*. (Paris,

2018), pp. 3973.

82.   V. Govindaraju, K. Young, A. A. Maudsley, Proton NMR chemical shifts and coupling constants for brain metabolites. *NMR in Biomedicine: An International Journal Devoted to the Development and Application of Magnetic Resonance In Vivo* **13**, 129-153 (2000).

83.   R. Kreis, C. S. Bolliger, The need for updates of spin system parameters, illustrated for the case of γ‐aminobutyric acid. *NMR in Biomedicine* **25**, 1401-1403 (2012).

84.   R. A. Edden, N. A. Puts, A. D. Harris, P. B. Barker, C. J. Evans, Gannet: A batch‐processing tool for the quantitative analysis of gamma‐aminobutyric acid–edited MR spectroscopy spectra. *Journal of Magnetic Resonance Imaging* **40**, 1445-1452 (2014).

85.   J. Ashburner, K. J. Friston, Unified segmentation. *Neuroimage* **26**, 839-851 (2005).

86.   T. Ernst, R. Kreis, B. Ross, Absolute quantitation of water and metabolites in the human brain. I. Compartments and water. *Journal of Magnetic Resonance, Series B* **102**, 1-8 (1993).

87.   S. W. Provencher, LCModel & LCMgui user's manual. *LCModel Version* **6**, (2014).

88.   A. L. Peek, T. Rebbeck, N. A. Puts, J. Watson, M.-E. R. Aguila, A. M. Leaver, Brain GABA and glutamate concentrations across pain conditions: A systematic literature review and meta-analysis of 1H-MRS studies using the MRS-Q quality assessment tool. *NeuroImage* **210**, 116532 (2020).

89.   R. Kreis, Issues of spectral quality in clinical 1H‐magnetic resonance spectroscopy and a gallery of artifacts. *NMR in Biomedicine* **17**, 361-381 (2004).

90.   M. Wilson, O. Andronesi, P. B. Barker, R. Bartha, A. Bizzi, P. J. Bolan, K. M. Brindle, I. Y. Choi, C. Cudalbu, U. Dydak, Methodological consensus on clinical proton MRS of the brain: Review and recommendations. *Magnetic resonance in medicine* **82**, 527-550 (2019).

interests. **Data availability:** Data from this study are available on request.

Figure captions

Fig. 1 Medial occipital ^{1}H-MRS voxel position. (a) axial view; (b) sagittal view and (c) coronal view; A anterior, P posterior, L left, R right, S superior, I inferior. Voxel dimensions LR: 30 mm; AP: 30 mm; SI: 25 mm; 22.5 mL.

Fig. 2 Sample visual stimuli. The stimuli consist of circular flickering Gabor grating foreground (F) and a static background (B), under specific configurations: (a) [F30, B0]; (b) [F100, B0]; (c) [F30, B100]; (d) [F100, B100].

Fig. 3 The scatter plots of θ values of the six participant groups: (a) Control_P (N = 21); (b) Control_L (N = 17); (c) Control_H (N = 12); (d) ASD_P (N = 17); (e) ASD_L (N = 13); (f) ASD_H (N = 14). The x-axis indicates the stimulus condition. 'B', background contrast; 'F', foreground contrast. The y-axis shows the θ value, which is the SSVEP increase relative to SSVEP under the zero foreground contrast with the same background.

Fig. 4 Scatter plots of the surround suppression (SS) on SSVEP responses to foreground by background interference for both the control and ASD groups at placebo. t, independent-sample t test value (d = 36); p, statistical significance value, corrected for multiple comparisons using Benjamini-Hochberg method.

Fig. 5 Scatter plot showing the correlation between GABA+ concentrations and θ[F100, B100] at placebo for both the control (N = 18) and ASD (N = 15) groups. *r*, pearson's linear correlation coefficient; *p*, statistical significance value.

Fig. 6 The individual sensitivity index Δθ was increased by arbaclofen in ASD group. *t*, independent-sample t test value (d = 12); *p*, statistical significance value.

Tables

Table 1 Stimulus configurations.

Stimulus configuration	Foreground contrast (FC)	Background interference (BI)
1	0%	0
2	30%	0
3	100%	0
4	0%	maximum
5	30%	maximum
6	100%	maximum

Table 2 LMM statistics for the six participant subgroups

Group (N)	BI		FC		Gender	
	es	p	es	p	es	p
Control_P (21)	-0.27	1.64e-06	0.17	0.002	0.01	0.85
Control_L (17)	-0.26	2.18e-04	0.16	0.021	-0.09	0.31
Control_H (12)	0.13	0.086	0.1	0.17	0.13	0.33
ASD_P (17)	0.022	0.71	-0.006	0.92	-0.01	0.91
ASD_L (13)	0.13	0.058	0.14	0.038	-0.08	0.56
ASD_H (14)	-0.28	3.88e-06	0.14	0.012	0.04	0.52

Abbreviations: N, number of participants*; BI,* background interference; *FC,* foreground contrast;

es, LMM estimated value; p, statistical significance.

Table 3 SVM classification and permutation testing results

Participant group pairs (N)			ca	p
Control_P (21)	vs.	Control_L (17)	57.5%	0.292
		Control_H (12)	78.5%	0.013
		ASD_P (17)	70.5%	0.033
		ASD_L (13)	64%	0.154
		ASD_H (14)	52%	0.442
Control_L (17)	vs.	Control_H (12)	66.5%	0.153
		ASD_P (17)	60%	0.273
		ASD_L (13)	64.5%	0.169
		ASD_H (14)	57%	0.285
Control_H (12)	vs.	ASD_P (17)	48%	0.607
		ASD_L (13)	30%	0.904
		ASD_H (14)	72.5%	0.021
ASD_P (17)	vs.	ASD_L (13)	54.5%	0.487
		ASD_H (14)	73%	0.038
ASD_L (13)	vs.	ASD_H (14)	76%	0.026

The p-values have been corrected using the MaxT procedure.
p<0.05 indicated significant statistical difference.

Table 4 Correlations between GABA+ and SSVEP for both groups at placebo

GABA+ (N)	SSVEP	r	p
Control (18)	θ[F30, B100]	-0.34	0.16
	θ[F100, B100]	0.49	0.039
ASD (15)	θ[F30, B100]	0.41	0.12
	θ[F100, B100]	0.11	0.7

Abbreviations: N, number of participants*; ϑ,* SSVEP response; *r,* correlation coefficient; *p,*

statistical significance.

Table 5 Participant demographic data and ASD clinical scores

Measure	Control	ASD	Effect size	p
Number (male / female)	12 / 13	11 / 8	0.42	0.52
Age	30.4 ± 9.1	37.3 ± 10.0	2.38	0.02
Full-scale IQ	118.8 ± 10.5[a]	116.5 ± 9.3[b]	0.7	0.49
AQ	17 ± 7.7[c]	36.8 ± 6.6	8.9	3.78e-011

Values are shown as means ± SD. Statistical results for the group difference of age, IQ and AQ (Autism Quotient) scores are the outcome of independent-sample t tests; and comparison of proportion of males and females carried out using Chi-squared test. As a result of Covid lockdown restrictions it was not possible to complete in-person IQ testing on [a] 2 controls; [b] 3 autistics. [c] One control participant changed email address, AQ data not returned.

SUPPLEMENTARY MATERIALS

Supplementary Materials and Methods

^{1}H-MRS – metabolite quantification and data quality control. For ^{1}H-MRS

analysis, there were 33 placebo visits (15 ASD, 18 controls), 27 low-dose visits (11

ASD, 16 controls), and 24 high-dose visits (11ASD, 13 controls) available. Eleven

ASD and 12 control participants completed all 3 visits. GABA+ metabolite measures

were determined with LCModel which uses a priori knowledge of the expected

individual spectra of several individual metabolites, i.e. basis sets, and fits the model

to the experimentally obtained spectra (*78, 79*). The basis set for the current work was

simulated in FID-A using high-density matrix simulations with 201 x 201 x 201

positions (*80, 81*). Each individual metabolite spectrum was obtained using published

chemical shifts and J-coupling constants (*82*) with updated values for GABA+ (*83*).

HERMES implementation and parameters combination were used for the simulations,

providing optimised spectral fitting and quantification. Basis set for the GABA

difference spectrum included GABA+, glutamate, glutamine, n-acetylaspartate,

n-acetylaspartilglutamate and glutathione. The water unsuppressed spectrum was used

as internal reference (i.e. water-scaling) and to perform eddy current correction.

The HERMES voxel was coregistered to the SPGR anatomical scan in MATLAB

9.2.0 (The Mathworks Inc., Natick, Massachusetts, USA) using the standalone

coregistration routine from Gannet 3.0 (*84*), which then runs the Statistical Parametric

Mapping 12 (SPM12) segmentation algorithm (*85*) to extract the proportion of grey

matter (pGM), white matter (pWM) and cerebrospinal fluid (pCSF) within the voxel. These tissue proportion values were then used to correct the water-scaled metabolite values for partial volume effect and different amounts of 'visible' water in each tissue type (accounting for possible confounds of different tissue proportions within the voxel). Each individual metabolite was corrected using the following calculation:

$$Met_{corr} = Met_{LCM} \frac{(43300 * pGM + 35880 * pWM + 55556 * pCSF) / 35880}{(1 - pCSF)} \quad (1S)$$

where Met_{corr} is the corrected metabolite value, Met_{LCM} is the original metabolite value obtained from LCModel, 43300, 35880, and 55556 are the concentrations (in mM) of water in GM, WM, and CSF, respectively (86). The division by 35880 in the numerator corrects for the initial LCModel analysis that assumes a purely white matter voxel during quantification (87). Finally, only the attenuation factor of water at TE=80ms was taken into account during quantification by inputting ATTH2O=0.37 in the analysis parameters (87), no other T1 or T2 relaxation times were taken into account and, thus, metabolites are reported in institutional units (iu).

Spectra were visually inspected to ensure only good quality datasets were included in the analysis. Briefly, spectra were visually inspected for artifacts (ghosts, subtraction artifacts), baseline irregularities and residuals. Both the quality procedures and measures reported followed published guidelines (88-90).

A 2 x 3 split-plot ANOVA with group (ASD, control) as between-subject factor and drug (placebo, low-dose and high-dose) as within-subject factor showed that there was no main effect of drug [$F(2, 42) = 1.173$, $p = 0.319$, $\eta2 = 0.053$] or group x drug

interaction [F(1.6, 42) = 0.735, p = 0.486, η2 = 0.034] of arbaclofen in occipital GABA+ concentrations (Fig. 1S).

Data quality measures and voxel tissue composition were compared between groups using two-tailed independent sample t test or Mann-Whitney U test, for normally and non-normally distributed variables (as assessed by the Shapiro-Wilk test), respectively. Level of significance was set to p < 0.05. Table S1 summarizes data quality measures and voxel composition with the respective test statistics. All quality metrics indicate very good data quality overall across both groups. Despite some between group differences in the signal-to-noise (SNR) and full-width-half-maximum (FWHM) at the active drug condition, there were no differences in the % CRLB estimates, which are normally used as an indicator of metabolite concentration estimations error and are influence both by the SNR and FWHM (*89, 90*). Here, GABA+ error estimates were all below 11% which indicate very good metabolite concentration estimation which were similar across groups. Hence, data quality did not likely influence the main findings. There were differences in the % of cerebrospinal fluid at placebo and % of grey matter at 15 mg. All metabolite concentrations were corrected taking voxel composition into account as per equation 1S, thus tissue differences did not drive the main findings.

EEG data processing

For the usable epochs, the selected channels (i.e. Oz, O1, O2, POz, PO3 and PO4) were far away from eyes thus rarely affected by eye movements; and we used a

relatively loose exclusion threshold (40 µV). As a result, all of the 60 epochs in each

participant visit were included in the analysis, i.e., there was no difference in the

number of usable epochs per visit between groups or across drug doses.

We also measured interaction effects for both the control (n = 21) and ASD (n =

17) groups at placebo. There was a significant interaction effect between background

interference (BI) and group (es = 0.29, p = 0.0002), and also between foreground

contrast (FC) and group (es = -0.17, p = 0.028). Thus, both the response to foreground

and its modulation by background interference were significantly different between

the two groups.

Supplementary Figures
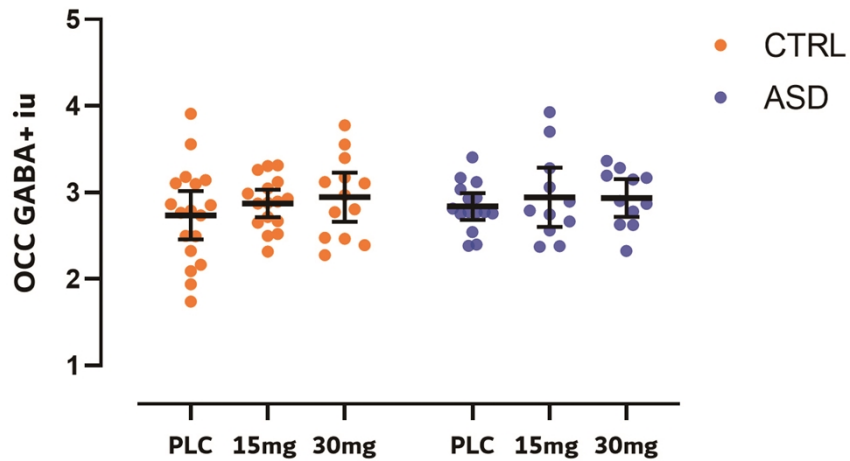
Fig. S1. Medial occipital GABA+ concentrations for both groups at all experimental conditions. Dots represent individual metabolite concentrations and bars represent mean ± 95 % confidence interval. GABA+, γ-aminobutyric acid + macromolecules; iu, institutional units; CTRL, control; ASD, Autism Spectrum Disorder, PLC, placebo, 15 mg, 15 mg arbaclofen; 30 mg, 30 mg arbaclofen.
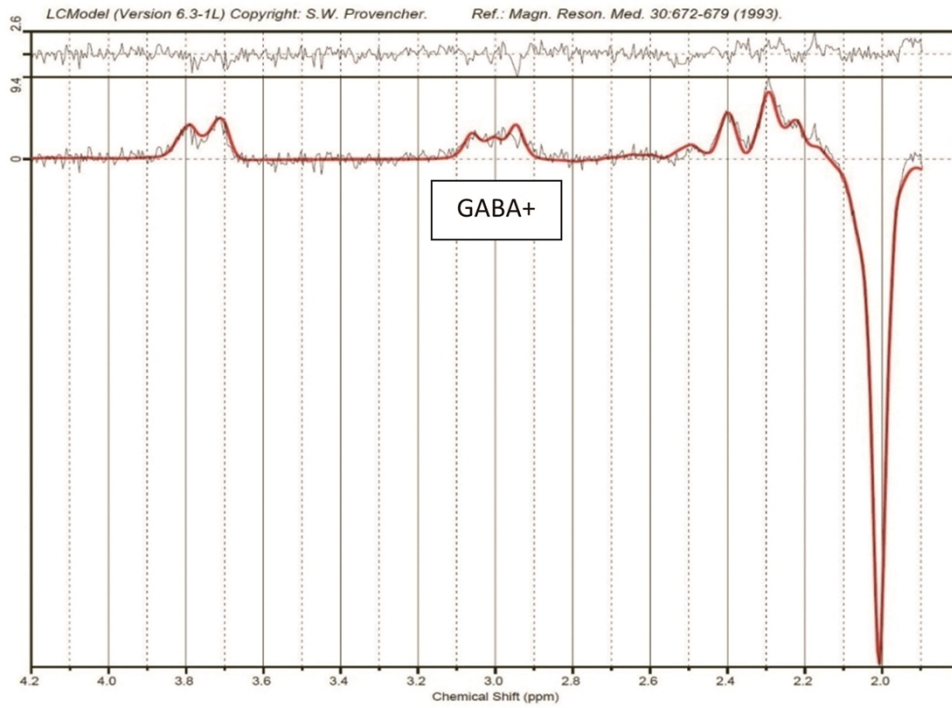
Fig. S2. Medial occipital GABA+ representative spectrum; GABA+, γ-aminobutyric acid + macromolecules; ppm, parts per million.

Supplementary Tables

Table S1. 1H-MRS data quality indicators and voxel tissue composition for the two groups with corresponding between-group comparisons for the GABA-difference spectra.

		CTRL		ASD		Statistics
		N = 18 (8m / 10 f)		N = 15 (10m / 5f)		
		mean ± SD	range	mean ± SD	range	
PLC	SNR	38 ± 7	28 - 49	36 ± 5	26 - 43	t(31) = 0.859; *p* = 0.411
	FWHM	0.042 ± 0.005	0.029 – 0.053	0.044 ± 0.005	0.033 – 0.048	U = 166.5 ; *p* = 0.259
	% CRLB GABA+	5 ± 2	4 - 11	5 ± 1	4 - 8	U = 104.5 ; *p* = 0.274
	pGM	0.67 ± 0.05	0.57 – 0.74	0.64 ± 0.04	0.58 – 0.72	t(31) = 1.191 ; *p* = 0.243
	pWM	0.24 ± 0.04	0.19 – 0.31	0.23 ± 0.02	0.18 – 0.27	t(31) = 0.382 ; *p* = 0.705
	pCSF	0.10 ± 0.02	0.07 – 0.13	0.12 ± 0.03	0.06 – 0.13	**t(31) = - 2.462 ; *p* = 0.020**
		N = 15 (5m / 10 f)		N = 11 (8m / 3f)		
		mean ± SD	range	mean ± SD	range	
15 mg	SNR	43 ± 7	32 - 53	34 ± 6	20 - 42	**t(24) = 3.534; *p* = 0.002**
	FWHM	0.041 ± 0.006	0.033 – 0.057	0.046 ± 0.005	0.038 – 0.053	**U = 122 ; *p* = 0.041**
	% CRLB GABA+	4 ± 1	4 - 5	5 ± 1	4 - 6	U = 97.5 ; *p* = 0.443
	pGM	0.68 ± 0.04	0.59 – 0.73	0.64 ± 0.04	0.58 – 0.74	**t(24) = 2.217 ; *p* = 0.036**
	pWM	0.22 ± 0.03	0.19 – 0.30	0.24 ± 0.03	0.18 – 0.27	t(24) = -1.647 ; *p* = 0.113
	pCSF	0.10 ± 0.02	0.07 – 0.16	0.11 ± 0.04	0.05 – 0.16	t(24) = -1.320 ; *p* = 0.199
		N = 12 (5m / 7 f)		N = 11 (8m / 3f)		
		mean ± SD	range	mean ± SD	range	
30 mg	SNR	39 ± 8	20 - 49	33 ± 3	29 - 47	**U = 28.5 ; *p* = 0.019**
	FWHM	0.041 ± 0.005	0.033 – 0.048	0.045 ± 0.005	0.038 – 0.053	t(21) = -1.661; *p* = 0.112
	% CRLB GABA+	4 ± 1	4 - 6	5 ± 1	4 - 8	U = 93.5 ; *p* = 0.091
	pGM	0.68 ± 0.05	0.57 – 0.73	0.65 ± 0.04	0.57 – 0.74	t(21) = 1.201 ; *p* = 0.243
	pWM	0.24 ± 0.05	0.18 – 0.30	0.23 ± 0.03	0.19 – 0.27	t(21) = 0.483 ; *p* = 0.634
	pCSF	0.10 ± 0.03	0.06 – 0.16	0.12 ± 0.04	0.06 – 0.17	t(21) = - .637 ; *p* = 0.117

Abbreviations: N, number of participants; *SD,* standard deviation; t, independent samples t test value; *U,* Mann–Whitney test value; *p,* statistical significance value; SNR, signal to noise ratio; FWHM, full width half maximum; %CRLB, percentage of the Cramer-Rao Lower Bounds standard deviation estimates; pGM, proportion of grey matter; pWM, proportion of white matter; pCSF,

proportion of cerebrospinal fluid; PLC, placebo, 15 mg, 15 mg arbaclofen; 30 mg, 30 mg arbaclofen. Statistically significant difference is in bold.

Table S2. ^{1}H-MRS GABA+ concentration, spectra quality metrics, and voxel tissue proportion for both groups at each drug condition

Control_P

Subject ID (N = 18)	GABA+ iu	SNR	FWHM	% CRLB GABA+	pGM	pWM	pCSF
Control 2	2.499	42	0.043	5	0.66	0.25	0.10
Control 3	2.766	34	0.048	5	0.63	0.26	0.11
Control 4	1.937	47	0.029	7	0.67	0.20	0.13
Control 6	2.164	42	0.048	6	0.70	0.22	0.08
Control 7	2.496	43	0.033	5	0.69	0.24	0.07
Control 8	3.908	28	0.043	4	0.73	0.19	0.08
Control 9	2.865	49	0.038	4	0.71	0.22	0.07
Control 11	3.559	29	0.043	4	0.62	0.25	0.13
Control 14	1.738	34	0.038	11	0.70	0.19	0.12
Control 15	2.323	38	0.043	5	0.64	0.29	0.07
Control 16	2.854	43	0.038	4	0.66	0.24	0.10
Control 17	2.791	47	0.043	4	0.65	0.26	0.09
Control 19	3.181	30	0.053	4	0.62	0.27	0.12
Control 20	2.091	31	0.043	7	0.57	0.31	0.12
Control 21	3.096	32	0.043	4	0.74	0.20	0.06
Control 22	2.736	37	0.038	5	0.67	0.23	0.09
Control 23	3.141	39	0.043	5	0.71	0.19	0.10
Control 24	3.107	37	0.043	4	0.63	0.25	0.12

Control_L

Subject ID	GABA+ iu	SNR	FWHM	% CRLB GABA+	pGM	pWM	pCSF

(N = 15)							
Control 2	2.988	42	0.033	4	0.66	0.24	0.10
Control 3	2.667	38	0.048	5	0.70	0.19	0.11
Control 4	3.045	53	0.038	4	0.67	0.21	0.12
Control 6	2.871	39	0.057	5	0.71	0.20	0.09
Control 7	3.313	41	0.038	4	0.69	0.23	0.08
Control 8	2.894	36	0.043	5	0.73	0.20	0.07
Control 9	2.927	50	0.043	4	0.71	0.19	0.09
Control 11	2.716	35	0.048	5	0.59	0.29	0.12
Control 14	2.315	47	0.038	5	0.71	0.19	0.10
Control 15	3.121	37	0.043	5	0.67	0.27	0.07
Control 16	2.498	50	0.043	4	0.68	0.23	0.09
Control 17	2.522	51	0.038	4	0.63	0.28	0.09
Control 22	3.262	32	0.038	4	0.68	0.22	0.09
Control 23	2.650	46	0.033	4	0.73	0.20	0.07
Control 24	2.881	44	0.038	4	0.63	0.22	0.16

Control_H

Subject ID (N = 12)	GABA+ iu	SNR	FWHM	% CRLB GABA+	pGM	pWM	pCSF
Control 2	2.772	49	0.043	4	0.67	0.23	0.11
Control 4	2.464	45	0.033	6	0.64	0.20	0.16
Control 6	3.107	31	0.048	4	0.71	0.20	0.10
Control 7	3.173	38	0.038	4	0.70	0.21	0.09
Control 8	3.552	31	0.043	4	0.72	0.20	0.08
Control 11	3.776	20	0.048	5	0.58	0.30	0.13
Control 14	2.390	42	0.038	4	0.73	0.18	0.08
Control 15	2.806	39	0.043	4	0.63	0.30	0.07
Control 16	2.475	49	0.033	5	0.70	0.24	0.06
Control 17	2.970	43	0.043	4	0.63	0.28	0.09
Control 22	3.400	36	0.048	4	0.68	0.21	0.11

Control 23	3.122	41	0.038	4		0.71	0.29	0.09

ASD_P

Subject ID (N = 15)	GABA+ iu	SNR	FWHM	% CRLB GABA+	pGM	pWM	pCSF
ASD 1	2.543	28	0.033	8	0.67	0.19	0.15
ASD 4	3.120	38	0.038	4	0.63	0.25	0.13
ASD 6	2.938	41	0.043	4	0.62	0.25	0.13
ASD 7	2.384	39	0.038	5	0.66	0.25	0.09
ASD 8	3.036	33	0.048	4	0.70	0.22	0.08
ASD 9	3.168	34	0.048	4	0.58	0.27	0.16
ASD 10	2.769	40	0.038	4	0.71	0.23	0.06
ASD 11	2.926	36	0.043	5	0.58	0.26	0.16
ASD 12	2.812	37	0.048	4	0.64	0.25	0.11
ASD 13	3.407	34	0.048	4	0.62	0.22	0.15
ASD 15	2.400	43	0.048	4	0.68	0.22	0.11
ASD 16	2.753	36	0.048	4	0.62	0.22	0.16
ASD 17	2.774	26	0.048	6	0.60	0.27	0.13
ASD 18	2.759	41	0.038	5	0.72	0.20	0.08
ASD 19	2.775	37	0.048	4	0.66	0.21	0.13

ASD_L

Subject ID (N = 11)	GABA+ iu	SNR	FWHM	% CRLB GABA+	pGM	pWM	pCSF
ASD 1	3.701	20	0.048	6	0.66	0.18	0.16
ASD 4	2.666	40	0.038	5	0.63	0.26	0.12
ASD 6	3.926	28	0.048	4	0.63	0.27	0.10
ASD 7	2.560	37	0.048	5	0.65	0.23	0.12
ASD 8	3.279	28	0.048	4	0.67	0.27	0.07
ASD 9	2.747	34	0.048	5	0.58	0.26	0.16
ASD 10	2.893	39	0.038	5	0.74	0.22	0.05

ASD 11	3.061	33	0.048	4	0.59	0.27	0.14
ASD 12	2.791	42	0.043	4	0.66	0.25	0.09
ASD 13	2.374	33	0.053	5	0.63	0.25	0.12
ASD 19	2.378	36	0.043	4	0.67	0.23	0.10

ASD_H

Subject ID (N = 11)	GABA+ iu	SNR	FWHM	% CRLB GABA+	pGM	pWM	pCSF
ASD 1	3.282	29	0.038	5	0.65	0.20	0.15
ASD 4	2.867	36	0.038	5	0.63	0.24	0.13
ASD 6	2.779	34	0.048	4	0.67	0.19	0.15
ASD 7	3.149	30	0.043	5	0.67	0.23	0.10
ASD 8	2.323	36	0.053	5	0.68	0.25	0.07
ASD 9	3.196	29	0.048	5	0.57	0.27	0.16
ASD 10	2.628	37	0.043	5	0.74	0.20	0.06
ASD 11	2.901	34	0.043	5	0.62	0.21	0.17
ASD 12	3.167	36	0.043	4	0.64	0.26	0.10
ASD 13	3.364	29	0.048	5	0.64	0.23	0.13
ASD 19	2.624	37	0.048	4	0.67	0.24	0.09

Table S3. The SSVEP value θ at different stimulus conditions for both groups at each drug condition

Control_P

Subject ID (N = 21)	θ			
	[F30, B100]	[F100, B100]	[F30, B0]	[F100, B0]
Control 2	0.00291303	0.136912193	0.450823764	0.832251623
Control 3	0.09612555	0.080431584	0.068038879	0.626643796
Control 4	-0.0046729	-0.002336449	0.150900038	0.392186902
Control 5	0.04170905	0.482706002	0.01369863	0.099867433
Control 6	0.00577201	-0.232323232	0.088130413	0.131431482
Control 7	0.09141531	0.212529002	0.245272825	0.930307942
Control 8	0.16129032	0.1617866	0.072457627	0.297881356
Control 9	0.21522843	0.269543147	0.116584565	0.775588396
Control 10	-0.2826167	-0.120543918	0.099447514	0.609241587
Control 11	0.10716002	0.563671312	0.196147799	0.297562893
Control 14	0.4513414	-0.012624934	-0.156653316	-0.02892746
Control 15	0.20554577	-0.055017606	0.303525805	0.778231988
Control 16	0.0016835	0.083754209	0.958629606	1.070458953
Control 17	-0.0350955	-0.159484673	0.20174482	0.234460196
Control 19	-0.0261369	0.370502007	0.042108155	0.234133056
Control 20	0.15137153	-0.060975056	0.179588132	1.006135988
Control 21	0.01267097	-0.172721166	0.442622312	0.583968683
Control 22	0.02889324	0.524975514	0.125232256	0.199554069
Control 23	-0.09897	-0.069413345	-0.037083333	0.05875
Control 24	-0.2102091	0.009571074	0.439399769	0.462870335

12

| Control 25 | 0.33907363 | 0.178147268 | 0.385251551 | 0.846312888 |

Control_L

Subject ID (N = 17)	θ			
	[F30, B100]	[F100, B100]	[F30, B0]	[F100, B0]
Control 2	0.2135388	0.488717666	0.702137998	0.776482021
Control 3	-0.2200108	-0.188273265	1.050241546	0.851207729
Control 4	0.19757366	0.514153668	0.223327306	0.297468354
Control 5	0.10076857	0.220324509	0.049751244	0.142017187
Control 6	0.02206897	0.66	0.091994382	0.962780899
Control 8	-0.258079	-0.055655296	0.033205005	0.060153994
Control 9	0.20203644	0.266881029	0.343402226	0.586645469
Control 10	-0.3276904	-0.203143894	-0.15301807	-0.12264514
Control 11	0.15220862	0.215007983	0.05370844	0.086104007
Control 12	0.06755515	0.134191176	0.044960474	0.12055336
Control 14	0.10028329	0.274220963	0.291102515	0.358317215
Control 16	-0.4529631	0.082884376	0.160055996	0.463835744
Control 17	-0.1829372	-0.227928693	0.760407816	1.281223449
Control 18	0.06479956	0.40911587	0.7824	0.0408
Control 22	-0.1899242	0.048149799	0.023275497	0.487092679
Control 24	0.32012579	0.441509434	0.013650546	0.225819033
Control 25	-0.2681661	-0.023875433	0.34715262	0.04738041

Control_H

Subject ID	θ

(N = 12)	[F30, B100]	[F100, B100]	[F30, B0]	[F100, B0]
Control 1	0.53588808	1.051094891	0.259792166	0.449240608
Control 3	0.48220516	0.856943475	-0.099341712	0.022740874
Control 4	0.19643917	0.208902077	0.176699029	0.185113269
Control 5	-0.4024226	-0.020188425	0.003957038	0.439231204
Control 6	0.45045558	-0.267084282	-0.564901793	-0.38001708
Control 7	-0.1248193	0.291566265	-0.115560061	0.092752154
Control 8	0.09674503	-0.087251356	0.053609342	0.078556263
Control 10	-0.1840986	-0.162840136	0.158969373	-0.03111327
Control 13	0.38178528	0.546441496	0.124790151	0.164521544
Control 14	0.58206687	0.828267477	0.31552795	0.408074534
Control 17	0.00319829	0.156183369	0.533213645	0.116098145
Control 23	-0.2180685	0.114745587	-0.070104287	-0.04345307

ASD_P

Subject ID (N = 17)	θ			
	[F30, B100]	[F100, B100]	[F30, B0]	[F100, B0]
ASD 1	0.75957728	0.49009247	0.482965932	0.394121576
ASD 2	-0.0361565	0.123823675	0.216111111	0.149444444
ASD 4	0.23391813	0.294346979	0.216526396	0.270084162
ASD 6	0.17386609	-0.030237581	0.082682591	0.134129536
ASD 7	-0.2920755	-0.288301887	0.176975945	0.304696449
ASD 8	0.6097561	0.121420997	0.09596929	0.103166987
ASD 9	0.07131537	0.147385103	-0.189905902	-0.13857998
ASD 10	0.40945365	0.179864948	0.000939408	0.231094411
ASD 11	0.2725896	0.557294296	0.519574306	-0.27708096
ASD 12	0.56460502	0.895284752	0.468480726	-0.00816327
ASD 13	0.51998074	-0.058257102	0.611460957	0.674433249
ASD 14	-0.0340271	-0.102081269	0.032413491	-0.13534823

ASD 15	-0.0260187	0.133290131	0.45037986	0.493633356
ASD 16	-0.3573703	-0.126846804	-0.219328957	0.028335767
ASD 17	-0.1815058	0.429229547	0.185602428	0.481045375
ASD 18	0.43501104	0.547723794	0.442856743	-0.01431351
ASD 19	0.47807713	0.344955098	-0.187103988	0.42527022

ASD_L

| Subject ID | θ | | | |
(N = 13)	[F30, B100]	[F100, B100]	[F30, B0]	[F100, B0]
ASD 1	0.31450828	0.108568647	0.309259259	0.622839506
ASD 2	0.31775181	0.376182526	-0.089481947	-0.31985871
ASD 3	0.20516214	0.862342819	0.667921687	1.260542169
ASD 4	0.12876852	0.825242718	0.415109667	0.450446791
ASD 5	0.2345954	0.384558278	-0.379351741	-0.31412565
ASD 7	0.45090376	0.1358085	0.086165049	0.214401294
ASD 8	0.62066182	1.040355125	0.103323263	0.857401813
ASD 10	0.05026455	-0.003174603	0.022445363	0.196692262
ASD 11	0.04070352	0.048743719	-0.197275923	-0.1370826
ASD 12	0.26409639	0.014939759	0.004923683	0.289512555
ASD 13	0.16122278	0.263819095	0.046296296	-0.04100529
ASD 14	0.3780707	0.209706411	0.295110594	0.218859139
ASD 19	0.0556042	0.33056042	-0.151857076	0.090267983

ASD_H

| Subject ID | θ | | | |
(N = 14)	[F30, B100]	[F100, B100]	[F30, B0]	[F100, B0]
ASD 1	0.20466445	-0.073774393	0.572146447	0.766690596
ASD 2	-0.2809105	-0.27884118	0.063009234	-0.02227051
ASD 3	-0.2232833	-0.114597544	0.146987952	0.123373494
ASD 4	-0.2241169	0.107998376	0.33409611	0.603203661

ASD 6	-0.0947274	0.317247542	0.108623154	0.294425917
ASD 7	-0.2367228	-0.289831606	0.201684605	0.605521759
ASD 8	0.15932066	-0.167408006	0.253640777	0.395024272
ASD 9	0.05582418	0.155164835	0.133944954	0.15412844
ASD 10	0.09881626	0.523417396	0.124288425	0.14516129
ASD 11	-0.0824317	0.492014426	0.102697998	0.224543081
ASD 12	-0.3657143	0.25978022	0.465419501	0.509070295
ASD 13	0.01851036	-0.154693698	0.269230769	0.638822115
ASD 14	0.16372141	-0.047817048	0.145342312	0.248597082
ASD 19	0.01316482	0.282253818	0.02130898	0.414003044